



## Reciprocating and fixed probe measurements of density and temperature in the DIII-D divertor

J.G. Watkins <sup>a,\*</sup>, R.A. Moyer <sup>b</sup>, J.W. Cuthbertson <sup>b</sup>, D.A. Buchenauer <sup>a</sup>, T.N. Carlstrom <sup>c</sup>,  
D.N. Hill <sup>d</sup>, M. Ulrickson <sup>a</sup>

<sup>a</sup> Sandia National Laboratories, Albuquerque, NM, USA

<sup>b</sup> University of California, San Diego, CA, USA

<sup>c</sup> General Atomics, San Diego, CA, USA

<sup>d</sup> Lawrence Livermore National Laboratory, Livermore, CA, USA

### Abstract

This paper describes divertor density and temperature measurements using both a new reciprocating Langmuir probe (XPT-RCP) which plunges vertically above the divertor floor up to the *X*-point height and swept, single, Langmuir probes fixed horizontally across the divertor floor. These types of measurements are important for testing models of the SOL and divertor which then are used to determine engineering design criteria for plasma facing components in reactor size tokamaks. The 6 mm diameter fixed single probes (19 domed and 2 flat at radially equivalent locations) are incorporated into the lower divertor floor at 19 radial locations and swept at 250 Hz. These probes are critical for determining plasma detachment from the floor during operation with high density, highly radiating divertors. By sweeping the divertor strike point across the fixed probes, different regions of the target plate incident flux profile can be sampled and a high resolution spatial profile can be obtained from each probe tip as the strike point moves past. The *X*-point reciprocating probe (XPT-RCP) provides  $n_e$  and  $T_e$  profiles with high spatial (2 mm) and temporal (0.5 ms) resolution from the target plate to the *X*-point along a single vertical chord at the same radial location as a fixed probe tip at a different azimuthal location. The probe  $n_e$  and  $T_e$  are compared to the divertor Thomson scattering (DTS)  $n_e$  and  $T_e$  (eight vertical points at 20 Hz,  $R_{\text{Thomson}} = R_{X\text{-point-rfp}}$ ). Recent observations have also shown divertor densities from  $3 \times 10^{19}$  to  $4 \times 10^{20} \text{ m}^{-3}$  near the target plate with the highest densities observed with  $\text{D}_2$  gas puffing. Electron temperature is typically of the order of 15–25 eV at the target rising to about 70 eV near the *X*-point. Lower temperature, higher density plasmas are observed along the inner leg. Generally good agreement among the XPT-RCP, the fixed floor probes, and the DTS is observed. Differences between these diagnostic measurements will also be discussed with respect to different operating regimes and conditions.

**Keywords:** DIII-D; Divertor plasma; Edge localized modes; Langmuir probe

### 1. Introduction

The divertor has become a central focus of interest in tokamak physics because of the ITER engineering design and the need to reduce or distribute the heat flux at the strike points. This design effort has relied on models of the divertor to predict conditions in the ITER divertor. The

models critically need new and more detailed divertor measurements under a variety of conditions. The geometry of the divertor in a toroidal tokamak is not very symmetric and we must have measurements and model calculations in two and three dimensions to fully describe the conditions there. To more fully address this area of study, we have recently implemented many new divertor diagnostics on DIII-D.

One diagnostic which has been used widely for measurements of density and electron temperature is the Langmuir probe. A fast reciprocating Langmuir probe was installed on the DIII-D midplane in 1990 [1] to study

\* Corresponding author. Present address: General Atomics 13-350, P.O. Box 85608, San Diego, CA 92186-5608, USA. Tel.: +1-619 455 3670; fax: +1-619 455 2266; e-mail: jon.watkins@gat.com.

profiles and fluctuation driven transport in a collaboration with a group at UCLA (now at UCSD). A fixed Langmuir probe array has been used on the divertor floor of DIII-D for several years [2] and it samples plasma conditions at 19 radial locations poloidally and several toroidal locations as well. A new reciprocating Langmuir probe [3] has been added to measure plasma conditions vertically above the divertor floor to obtain density and temperature probe measurements along the field lines away from the floor. These two probe systems complement a new divertor Thomson scattering system [4] which measures vertically at the same radius as the reciprocating probe but at a different toroidal location. In this paper, we present an overview of our new divertor probe measurements and how they compare with the new divertor Thomson scattering system.

Langmuir probes have both advantages and disadvantages. The main advantages of probes are the spatial and temporal resolution and the ease of use and placement. The main disadvantages are the uncertainties in the theory of data interpretation, perturbations on the plasma, and erosion of the probes by the high heat fluxes in the tokamak. Some new theories have been developed recently [5–7] to help in the interpretation of probe data. Our new probes incorporate domed collector tips made of various types of high thermal conductivity graphite to increase the power limits they can handle and to extend the lifetime of the probe in the tokamak. Our new reciprocating probe, for instance, can operate in DIII-D with up to 10 MW of

auxiliary heating and can measure the time evolution of ELM events and survive disruptions as well. The divertor probe fixed array has been upgraded to this same type of new 1D graphite fiber composite (Thermograph 8000).

## 2. Measurements

This section describes the density and temperature measurements in different zones of the DIII-D divertor made with our Langmuir probes and the comparison with the new divertor Thomson scattering system (DTS).

### 2.1. The strike point profiles

Sweeps of the divertor strike points utilize the shape control capabilities of DIII-D and allowed us to make divertor target plate measurements across the strike points with our fixed probes on the floor. Fig. 1 shows the density and temperature profiles across the divertor floor. Since we have many probes measuring in parallel (3 cm apart, 250 Hz), we can fill in a profile in 100–200 ms, depending on the speed of the sweep. This is similar to the time needed to get a reciprocating probe profile. The case shown here is for an L-mode plasma with strike point sweeping heated with 3.2 MW of neutral beam injection at a line averaged density of  $6.2 \times 10^{19} \text{ m}^{-3}$ . We can see that the density is about 1.5 times higher at the outer strike point and the temperature is 3–4 times lower at the inside

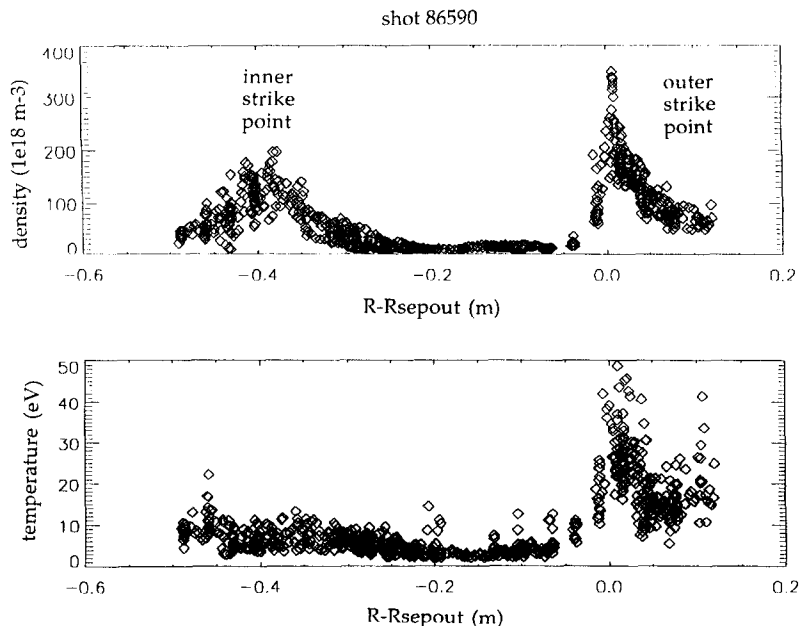


Fig. 1. Profiles of the density and temperature across the divertor floor obtained with the fixed probe array. The horizontal position ( $R - R_{\text{sepout}}$ ) is normalized to the outer strike point position. Sweeping the strike point allows us to construct this detailed profile from many fixed probe measurements.

strike point. These conditions are consistent with higher radiation and reduced heat flux measured on the inside divertor leg. The electron pressure is lower at the inner strike point which is typical of the highly radiating conditions approaching detachment that are normally found there without external pumping of the SOL. Fig. 2 shows a detail of the outer leg target plate profiles. The density and temperature peak at the strike point and decay exponentially away. For this case, the density decay length is 4.2 cm in the SOL and 1.7 cm in the private flux region. The temperature decay length is 3.0 cm in the SOL and 1.3 cm in the private flux region. The SOL/private flux ratio of these decay lengths is 2.5 for the density and 2.3 for the temperature. These fits were done including a flat pedestal on the profiles.

2.2. The upstream divertor leg profiles

The divertor reciprocating probe which scans vertically up from the lower divertor floor at  $R = 1.49$  m can penetrate the divertor leg from below, measure a profile, and measure the same profile again as the probe retracts

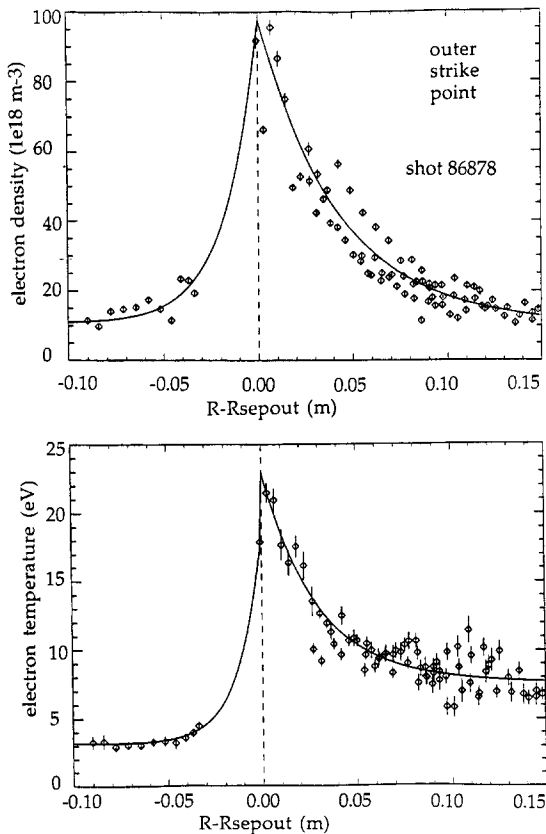


Fig. 2. Detailed outer strike point floor profiles normalized to the outer strike point position.

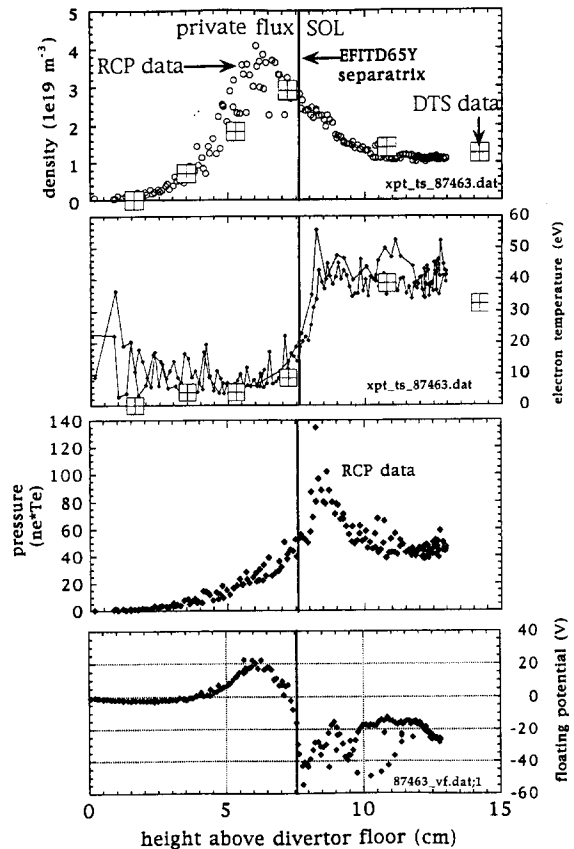


Fig. 3. Vertical profiles of the outer divertor leg obtained with the divertor RCP. The density peaks at a slightly different location from the temperature and the pressure. The floating potential drops significantly at the predicted separatrix and helps to locate it during operation of the probe.

(fixed strike points). We have also scanned across the leg at an angle as the strike point is swept. Fig. 3 shows a typical density and temperature profile obtained with the divertor RCP through the fixed outer divertor leg. The probe data retraces itself during the return stroke and agrees with divertor Thomson scattering measurements made before the probe plunge. This is an L-mode plasma similar to the previous one shown in Fig. 1. The density profile shows a peak slightly shifted from the peaks of the temperature and pressure profiles. The temperature profile rises outside the EFITD65Y separatrix (see below) and is a fairly constant 40 eV in the expanded flux region. The position of the pressure peak, mostly controlled by the temperature profile, is within 1 cm of the separatrix. The DTS system verifies these measurements but at lower spatial resolution.

The floating potential was found to be an accurate and convenient measure of the separatrix position. The steep negative drop in  $V_f$ , corresponding to the electron tempera-

ture increase, agrees with the outer leg divertor separatrix position calculated by EFITD65Y [8,9] if we use the finite edge current boundary condition. The zero edge current boundary condition results in a calculated separatrix position 3 cm higher and in a flat part of the profile. The raw floating potential data can be conveniently used to locate the separatrix during operation of the probe. This observation implies that the correct boundary condition for locating the separatrix in the divertor is to allow some edge current to flow. As further evidence for this boundary condition, we have observed electrical currents flowing near the separatrix and into the target plate with the fixed probe array.

### 2.3. ELM measurements

The 2 kHz measurement capability of the RCP probe systems allow us to characterize conditions during the edge localized modes (ELMs) in the divertor. Fig. 4 shows profile data obtained by the divertor RCP in the outer divertor SOL during ELMing H-mode. Since the ELMs, according to the photodiodes, were similar to within 20%, we can see how the ELMs affect the density at different heights above the divertor floor. The DTS points shown are all measured simultaneously at a time which did not coincide with an ELM and are indicative of the background density profile. The density pulses seen by the XPT-RCP during the ELMs represent nearly the same increment in the background density at different heights off the floor. Fig. 5 shows an example of how the density in the SOL 10 cm above the target plate varies with time during an ELM and how it compares to the  $D_\alpha$  light we see on the photomultiplier looking at the same region. The

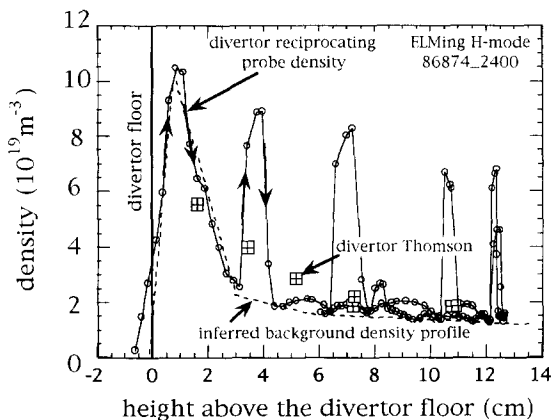


Fig. 4. SOL vertical density profile during ELMing H-mode. The ELMs are seen as large perturbations on the density as the probe travels vertically upward. In between the ELMs we can see portions of the unperturbed profile. The DTS vertical profile points are all measured simultaneously at a time that does not correspond to an ELM.

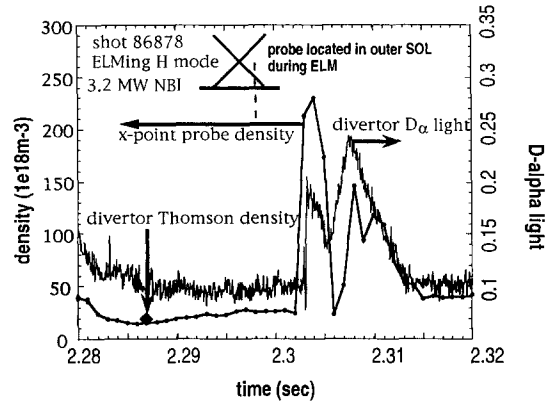


Fig. 5. The outer SOL ELM density and  $D_\alpha$  light show the same double peaked character. Both bursts of light are associated with increases in the local density. This  $D_\alpha$  monitor is looking through the SOL region where the probe tip is located at the time of the ELM.

double peaked time histories of the signals have the same character and therefore both peaks in the  $D_\alpha$  signal indicate a real increase in density. The proportionality between these signals is different for the second peak which indicates a change in  $T_e$  and/or the neutral particle density. We have also recently obtained fast (50 kHz) measurements of the profiles of the particle flux to the divertor floor during an ELM with our fixed probe array. From these measurements we see that the integrated particle flux distribution is unchanged [10] during the ELM even though the magnitude of this flux is increased.

### 2.4. DTS/probe comparison

The fixed and reciprocating probe systems and Thomson scattering in general have fairly good agreement. We have observed some disagreements of various types in cases from ohmic and H-mode (5 MW) plasmas. In partially detached divertor (PDD) discharges where the strike point particle flux drops significantly at the target plate and the SOL flux is enhanced, the DTS and floor probe measurements clearly do not agree. Good RCP data for comparison are not yet available under these conditions. The lowest DTS laser channel (1.6 cm above the floor) indicates  $2\text{--}3\times$  higher density and  $5\text{--}10\times$  lower temperature than the fixed floor probe at the same radial location. Electron temperatures are not expected to increase toward the divertor floor. Attempts to resolve this conflict with IR camera measurements were not conclusive because of low heat flux under non-ELMing conditions, ELMs at higher power, turbulence, and high amounts of radiated power in the divertor under these conditions. Single probe temperature measurements are known to be somewhat sensitive to the tail of the electron distribution function [11], however,

and these higher energy tail electrons may be more indicative of higher temperature conditions elsewhere along the field line. Presently, no attempt has been made to fit the electron saturation portion of the characteristic which could eliminate this sensitivity. The observed disagreement between the laser and probe during PDD is consistent with an erroneously high probe temperature and a low inferred probe density. The sensitivity of the probe  $T_e$  to high energy electrons, however, does not explain other types of disagreement where  $n$  or  $T$  agree and the other does not agree. In these cases, the predicted particle flux from DTS  $n_e$  and  $T_e$  measurements does not agree with the probe saturation current. Further, under the highly collisional PDD conditions, it is less likely for the non-Maxwellian high energy tail distribution to be a problem than under normal conditions where we often find good agreement between the two systems.

### 3. Results

We observe, for L-mode, that target plate radial gradients in the SOL are less steep than in the private flux region, the inner strike point is near detachment under normal (non-pumped) conditions, and that the density peak in the upper part of the divertor leg is slightly shifted from the temperature and pressure which peak further in the SOL outside the separatrix. In ELMing H-mode, the density increase associated with an ELM is nearly a constant increment above the background density at various heights off the floor. The double peak in the  $D_\alpha$  light seen occasionally during ELMs resembles the density measured locally but the proportionality changes for the second peak indicating lower  $T_e$  and/or increased neutral density. Comparisons among the floor probes, the reciprocating probe and the Thomson scattering system mostly agree except under conditions approaching detachment. The disagreements, however are not always consistent with an erroneously high  $T_e$  probe measurement.

### 4. Conclusions

Probes give measurements across the floor simultaneously and are very useful for high temporal and spatial resolution measurements. The fine structure of the gradients that we observe will be very useful in developing accurate models of the divertor. The fast time response of the probe measurements allows detailed study of ELMs. The ability to compare with laser measurements is a unique advantage and may yield some interesting facts about the accuracy of divertor measurements for future and present day fusion experiments.

### Acknowledgements

The valuable suggestions and support of Brian Labombard (MIT), Claude Boucher (CCFM), Arnie Kellman (GA), Dennis Whyte (CCFM/GA), Charles Lasnier (LLNL), Mike Brown (LLNL), and Bill Meyer (LLNL) are greatly appreciated. This work was supported by the U.S. Department of Energy under Contract Nos. DE-AC03-89ER5114, DE-AC04-94AL85000, W-7405-ENG-48 and Grant No. DE-FG03-95ER54292.

### References

- [1] J. Watkins et al., Rev. Sci. Instrum. 63 4728.
- [2] D. Buchenauer et al., Rev. Sci. Instrum. 61 2873.
- [3] J. Watkins et al., Rev. Sci. Instrum., to be published.
- [4] T. Carlstrom et al., Rev. Sci. Instrum., to be published.
- [5] M. Weinlich et al., IPP Report 5–64 (1995).
- [6] K. Guenther, in: Proc. of the 1995 Eur. Phys. Soc., p. I-433.
- [7] Q. Yu and J.A. Wesson, Plasma Phys. Controlled Fusion, JET-P(95)81.
- [8] L.L. Lao, H. St. John, R.D. Stambaugh and W. Pfeiffer, Nucl. Fusion 25 (1985) 1421.
- [9] L. Lao et al., Nucl. Fusion 30 (1990) 1035.
- [10] A. Leonard et al., these Proceedings, p. 628.
- [11] P.C. Stangeby, Plasma Phys. Controlled Fusion 37 (1995) 1031.